Pinhole X-ray Fluorescence Imaging of Gadolinium Nanoparticles: A Preliminary Monte Carlo Study

Seongmoon Jung [a,b], Wonmo Sung [a,b] , Sung-Joon Ye [a,c,d*]
[a]*Program in Biomedical Radiation Sciences, Department of Transdicsiplinary Studies, Graduate School of Convergence Science and Technology, Seoul National University, Seoul, Korea*
[b]*Biomedical Research Institute, Seoul National University Hospital, Seoul, Korea*
[c]*Interdisciplinary Program in Radiation Applied Life Science, Seoul National University College of Medicine, Seoul, Korea*
[d]*Department of Radiation Oncology, Seoul National University Hospital, Seoul, Korea*
[*]*Corresponding author: sye@snu.ac.kr*

1. Introduction

In recent years there has been increasing interest in the application of metal nanoparticles to cancer treatment and detection. Metal nanoparticles accumulated within tumors result in enhanced radiotherapy efficacy [1]. X-ray fluorescence imaging is a modality for the element-specific imaging of a subject through analysis of characteristic x-rays produced by exploiting the interaction of high atomic number elements and incoming x-rays. Previous studies have utilized a polychromatic x-ray source to investigate the production of *in vivo* x-ray fluorescence images for the assessment of concentrations and locations of gold nanoparticles [2]. However, previous efforts have so far been unable to detect low concentrations, such as 0.001% gold by weight, which is an expected concentration accumulated in tumors [3].

We examined the feasibility of a monochromatic synchrotron x-rays implementation of pinhole x-ray fluorescence imaging by Monte Carlo simulations using MCNP5 [4]. In the current study, gadolinium (Gd) nanoparticles, which have been widely used as a contrast agent in magnetic resonance imaging and also as a dose enhancer in radiation therapy, were chosen for tumor targeting. Since a monochromatic x-ray source is used, the increased x-ray fluorescence signals allow the detection of low concentrations of Gd. Two different monochromatic x-ray beam energies, 50.5 keV near the K_{edge} energy (i.e., 50.207 keV) of Gd and 55 keV, were compared by their respective imaging results.

2. Materials and Methods

2.1 Monte Carlo Simulation Geometry

In the Monte Carlo model, as shown in Fig.1, 1 cm diameter cylindrical columns containing water loaded with Gd nanoparticles (0.001-0.5% Gd by weight) were inserted into a 5 cm diameter cylindrical water phantom. The pinhole detection system consisted of a lead shield of 1 mm with a 4 mm diameter pinhole to allow good imaging spatial resolution. A detector plate was made up of 324 pixels, each of 2.5 mm^2. The water phantom was irradiated by fan beams of 50.5 keV and 55 keV photons. The fan beams were 5 cm in width and 0.1 cm in height to fully cover the phantom. The distance from the beam plane to pinhole, and from the pinhole to detector were both 2 cm.

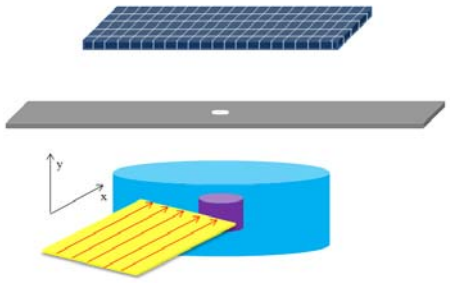

Fig. 1. Monte Carlo model.

2.2 Data Acquisition

K-characteristic x-rays are isotropically emitted from Gd nanoparticles due to photoelectric interactions with the monochromatic x-ray source. We focused on acquiring 42-44 keV peaks, corresponding to $K_{\alpha 1}$ and $K_{\alpha 2}$, to take advantage of the increased signal intensity (Fig. 2). X-ray fluorescence signals were obtained by selectively subtracting 42-44 keV photon flux of the water phantom (i.e. background signals) from the flux of the Gd column inserted in the water phantom by equation (1) and described in Fig. 3.

$$F_{sub} = F_{Gd+water} - F_{water} \quad (1)$$

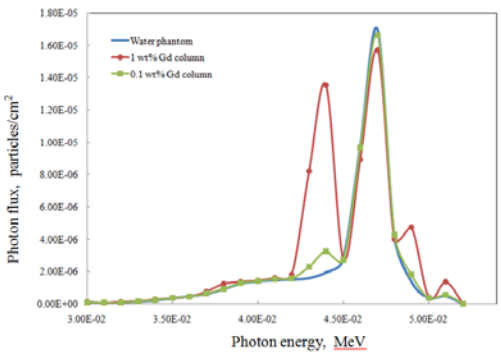

Fig. 2. Energy spectrum of the central pixel with and without Gd column.

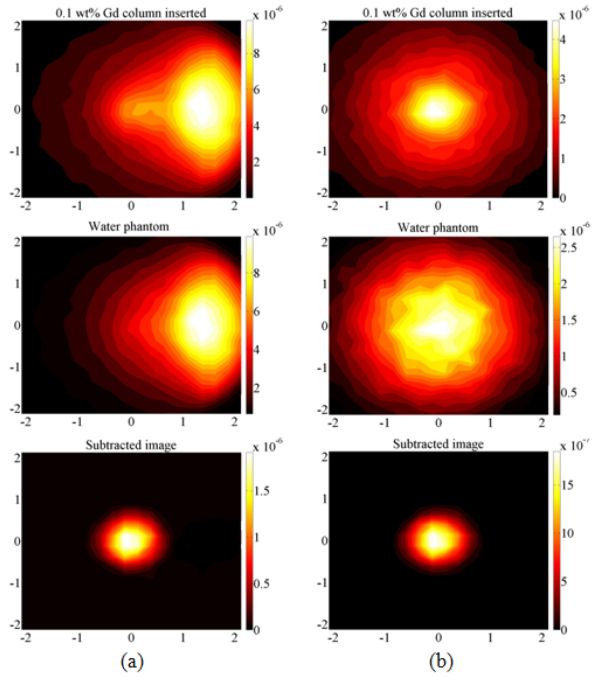

Fig. 3. The subtracted images were acquired by subtracting the flux of water phantom from the flux of the 0.1 wt% Gd column inserted in the water phantom. The phantoms were irradiated with 50.5 keV photon beam (a) and 55 keV photon beam (b).

2.3 Image processing

Attenuation correction was conducted for the primary beam through the phantom and Gd fluorescence *en route* to the detector plate by equation (2).

$$k_a = \frac{1}{e^{-\mu_{w,E} \cdot x} \cdot e^{-\mu_{w,K} \cdot y}} \quad (2)$$

k_a is the attenuation correction factor, and $\mu_{w,E}$ is the linear attenuation coefficient of water when the phantom is irradiated by photons of energy E. $\mu_{w,K}$ is the linear attenuation coefficient of water for the photons of K characteristic x-rays after the interaction. x is the path length of photons before the photoelectric interactions, and y indicates the path length of fluorescence photons after the interactions.

Also the effect of decreased fluorescence signals as distance from the central pixel of the detector plate increased was considered. It is caused by the inverse square law, and is an inherent geometrical limitation of pinhole detection systems. The correction factor, k_r is determined from empirical data using MCNP5 code. Corrected photon flux can be expressed as equation (3).

$$F = F_{sub} \cdot k_a \cdot k_r \quad (3)$$

2.4 Linearity

F values of the pixels expected to detect Gd nanoparticles could be integrated, since we know the locations of Gd columns. The linearity between the integrated F values and the Gd concentration in wt% was investigated.

3. Results

After data acquisition and image processing, x-ray fluorescence images of different concentrations of Gd columns were obtained as shown in Fig. 4. Analysis indicated a strong linear relationship between the Gd concentrations and integrated fluorescence photon flux from Gd columns, as displayed in Fig. 5.

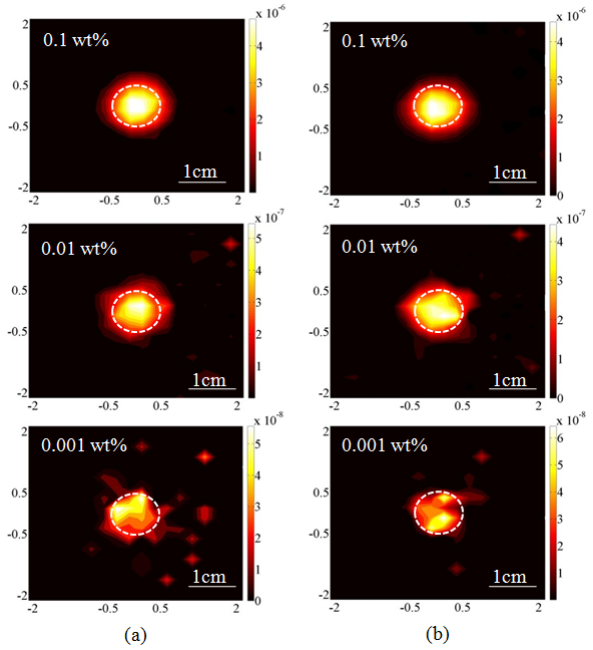

Fig. 4. The x-ray fluorescence images of 0.001 wt% - 0.1 wt% Gd columns inserted in water phantoms which were irradiated with 50.5 keV photon beam (a) and 55 keV photon beam (b).

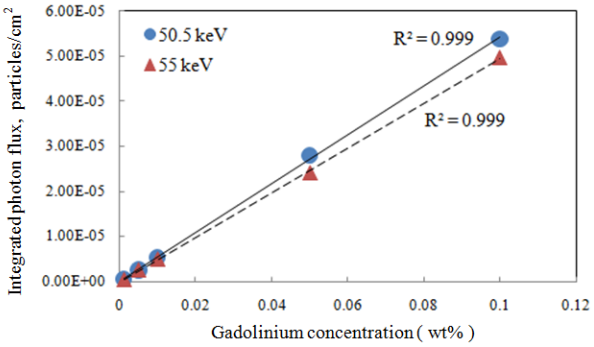

Fig. 5. Linear relationship between the concentration and integrated flux from 0.001 wt% to 0.1 wt% of Gd columns.

The images of three different locations and concentrations of Gd columns in water phantoms are shown in Fig. 6. The linearity between the concentration and integrated photon flux is shown in Fig. 7.

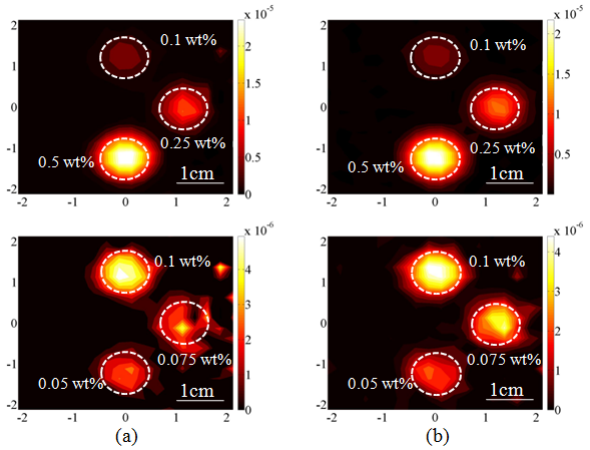

Fig. 6. The images of Three columns inserted water phantom irradiated with 50.5 keV photon beam (a) and 55 keV photon beam (b).

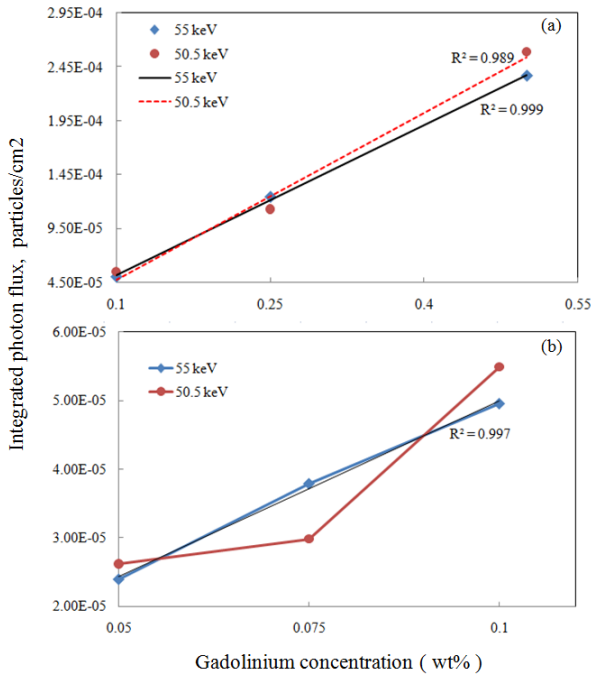

Fig. 7. Linear relationship between the concentration and integrated photon flux of 0.1 wt%, 0.25 wt% and 0.5 wt% columns (a) and 0.05 wt%, 0.075 wt% and 0.1 wt% columns (b).

4. Conclusions

Using Monte Carlo simulations the feasibility of imaging low concentrations of Gd nanoparticles (e.g., 0.001 wt%) with x-ray fluorescence using monochromatic synchrotron x-rays of two different energies was shown. In the case of imaging a single Gd column inserted in the center of a water phantom, the fluorescence signals from 0.05 wt% and 0.1 wt% Gd columns irradiated with a 50.5 keV photon beam were higher than those irradiated with 55 keV. Below 0.05 wt% region no significant differences were found.

However, the photon beam of 55 keV showed better images and linear relationship between the three different concentrations and locations Gd columns as described in Fig. 6 and Fig. 7. The poor results of the 50.5 keV photon beam are explained by the locations of the 0.25 wt% and 0.075 wt% Gd columns. Since these two columns were located in the position where the background photon signals are dominant, as seen in Fig. 3(a), a little change of water into Gd could reduce the flux, $F_{Gd+water}$ in equation (1).

REFERENCES

[1] J. F. Hainfeld, D. N. Slatkin and H. M. Smilowitz, The use of Gold Nanoparticles to Enhnace Radiotherapy in mice, Physics in Medicine and Biology, Vol.49, pp.N309 – N315, 2004.

[2] S. K. Cheong, B. L. Jones, A. K. Siddiqi, F. Liu, N. Manohar and S. H. Cho, X-ray Fluorescence Computed Tomography (XFCT) Imaging of Gold Nanoparticle-loaded Objects Using 110 kVp X-rays, Physics in Medicine and Biology, Vol.55, pp.647 – 662, 2010.

[3] N. Khlebstov and L. Dykman, Biodistribution and Toxicity of Engineered Gold Nanoparticles: A Review of *in vitro* and *in vivo* Studies, Chemical Society Reviews, vol.40, pp.1647 – 1671.

[4] X-5 Monte Carlo Team, MCNP – A General Monte Carlo N-Particle Transport Code, Version 5, LA-UR-03-1987, Los Alamos National Laboratory, 2003.